'94 KACC (1994. 10. 17 ~ 20)

인체형 로봇 메니퓰레이터의 동역학적 최적설계

이상헌*, 이병주**, 곽윤근*

* 305-701 대전시 유성구 구성동 373-1 한국과학기술원 정밀공학과
** 333-860 충남 천안우체국 사서함 55 한국기술교육대학 제어기계공학과

Dynamic Optimal Design of an Anthropomorphic Robot Manipulator

S.H. Lee*, B-J. Yi**, Y.K. Kwak*

* *Korea Advanced Institute of Science and Technology, Dept. of Precision Eng. and Mechatronics, 373-1 Kusong-dong, Yusong-gu, Taejon, 305-701 Korea*

** *Korea Institute of Technology and Education, Dept. of Mechanical Eng., San 37-1 Gajeon-ri, Byungchon-myon, Chonan-gun, Chungnam, 333-860 Korea*

Abstract

In this study, dynamic optimal design for a two degree-of-freedom anthropomorphic robot module is performed. Several dynamic design indices associated with the inertia matrix and the inertia power array are introduced. Analysis for the relationship between the dynamic parameters and the design indices shows that trade-offs exist between the isotropy and the dynamic design indices related to the actuator size. A composite design index is employed to deal with multi-criteria based design with different weighting factors, in a systematic manner. We demonstrate the fact that dynamic optimization is another significant step to enhance the system performances, followed by kinematic optimization.

1. Introduction

Previously, in the design of robot manipulators, much attention has been paid to the kinematic optimization for robot manipulators. Recently, dynamic performances have become other significant design factors with increase of the operational speed, and therefore dynamic optimal design is emphasized to achieve the improvement of dynamic performances(Youcef-Toumi and Asada, 1987; Park and Cho, 1991; Singh and Rastegar, 1992).

In this study, dynamic optimization for a two degree-of-freedom robot module as shown in Fig. 1 is performed. This module is anthropomorphic since it resembles the musculoskeletal structure of the human arm. The kinematic optimization has been carried out for the same robot module in the previous work by the present authors, and thus dynamic optimization starts from the results of the kinematic optimization. Several dynamic design indices associated with the inertia matrix and the inertia power array are introduced. To cope with a multi-criteria based optimal design, a concept of composite design index is employed. In this study, we demonstrate the fact that dynamic optimization is another significant step to enhance the system performance, followed by kinemtaic optimization.

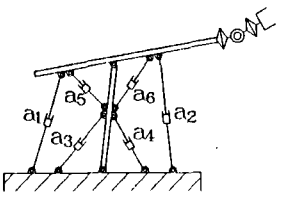

Fig. 1 Two degree-of-freedom anthropomorphic robot module

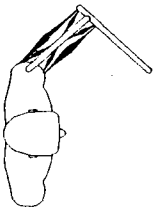

Fig. 2 Two-segment model of the upper limb

2. Musculoskeletal Structure of the Human Upper Extremity

The human arm consists of 29 muscles(Spence, 1986), showing redundancy in actuation compared to seven joint space and six operational space freedoms. It is presumed that the human arm utilizes these abundant force redundancies to optimize several objectives. Figure 2 illustrates the planar two-segment abstraction of the upper extremity(*e.g.*, the forearm and arm). In this conceptual model, the skeletal segments are considered to be rigid bodies and the muscles are each assumed to have a single point of origin and insertion.

Figure 1 denotes an anthropomorphic manipulator models which resembles the structure of Fig. 2. Each joint corresponds to the human muscle. Hogan(1985) investigated the spring-like behavior for this module. Yi and Freeman(1991) developed a mathematical model of the spring-like property for this module. In this study, optimal distribution of dynamic parameters of this manipulator is investigated in order to enhance the overall dynamic characteristics.

3. Kinematic/Dynamic Modeling

A kinematic constraint-embedding procedure(Kang *et al.*, 1990) is employed for explicit dynamic modeling of general closed-loop type robot systems in terms of a minimum coordinate set. The closed-loop manipulator is assumed to have an open-tree structure. By using

the principle of virtual work, the open-chain dynamics can be directly incorporated into the closed-chain dynamics.

3.1 Kinematic Modeling

The actuated joints and dependent joints are represented as $\underline{\Phi}_A$ and $\underline{\Phi}_d$, respectively, while the whole Lagrangian joints are given as $\underline{\Phi}_p$. For redundantly actuated closed-loop mechanisms, $\underline{\Phi}_A$ will be represented as follows:

$$\underline{\Phi}_A = [\underline{\Phi}_s^T, \underline{\Phi}_a^T]^T \tag{1}$$

where $\underline{\Phi}_a$ denotes the set of minimum coordinate and its dimension is the same as the degree-of-freedom of the system, and $\underline{\Phi}_s$ denotes the set of redundantly actuated joints.

The velocity vector for the whole Lagrangian joints is related to the set of minimum coordinate(Kang *et al.*, 1990) as

$$\dot{\underline{\Phi}}_p = [G_a^p]\,\dot{\underline{\Phi}}_a \tag{2}$$

where $[G_a^p]$ is the first order Kinematic Influence Coefficient(KIC) representing the relationship between $\dot{\underline{\Phi}}_p$ and $\dot{\underline{\Phi}}_a$. The velocity vector($\dot{\underline{u}}$) at the end effector is obtained by substituting the information of Eq. (2) into an open-chain kinematic relation, as

$$\dot{\underline{u}} = [G_a^u]\,\dot{\underline{\Phi}}_a \tag{3}$$

where $[G_a^u]$ is the first order KIC representing the relationship between $\dot{\underline{u}}$ and $\dot{\underline{\Phi}}_a$. Reversely, $\dot{\underline{\Phi}}_a$ can be represented as a function of $\dot{\underline{u}}$.

$$\dot{\underline{\Phi}}_a = [G_u^a]\,\dot{\underline{u}} = [G_a^u]^{-1}\,\dot{\underline{u}}. \tag{4}$$

An acceleration vector at the set of minimum coordinate is obtained by differentiating Eq. (4) with respect to time, as

$$\ddot{\underline{\Phi}}_a = [G_u^a]\,\ddot{\underline{u}} + \dot{\underline{u}}^T[H_{uu}^a]\,\dot{\underline{u}} \tag{5}$$

where $[H_{uu}^a]$ is the second order KIC representing the relationship between $\ddot{\underline{\Phi}}_a$ and $\dot{\underline{u}}$.

A force equilibrium equation between the force vector ($\underline{T}_u$) at the end effector and the force vector($\underline{T}_A$) at the actuating joints, is represented as

$$\underline{T}_u = [G_u^A]^T\underline{T}_A \tag{6}$$

where the first order KIC representing the relationship between $\underline{\Phi}_A$ and $\underline{u}$ is defined as

$$[G_u^A] = [G_a^A][G_u^a]. \tag{7}$$

In Eq. (7), $[G_a^A]$ is a subset of $[G_a^p]$. Since the column dimension of $[G_u^A]^T$ is greater than the row dimension, $\underline{T}_A$ has infinite solutions. In this study, $\underline{T}_A$ is obtained in such a way that the 2-norm $\|\underline{T}_A\|$ is minimized

$$\underline{T}_A = ([G_u^A]^+)^T\underline{T}_u = [G_A^u]^T\underline{T}_u \tag{8}$$

where $[G_A^u]$ is defined as

$$[G_A^u] = [G_u^A]^+ = ([G_u^A]^T[G_u^A])^{-1}[G_u^A]^T. \tag{9}$$

3.2 Dynamic Modeling

A dynamic model at the set of minimum coordinate is given as

$$\underline{T}_a = [I_{aa}^*]\,\ddot{\underline{\Phi}}_a + \dot{\underline{\Phi}}_a^T[P_{aaa}^*]\,\dot{\underline{\Phi}}_a \tag{10}$$

where $\underline{T}_a$ is the inertial force vector at the set of minimum coordinate. $[I_{aa}^*]$ is the inertia matrix, and $[P_{aaa}^*]$ is the inertia power array representing the effects of the coriolis force and the centrifugal force.

In the dynamic optimization procedure, we employ a dynamic equation which represents the relationship between the velocity/acceleration vector at the end effector and the actuating force vector. This can be obtained as Eq. (11) by using the coordinate transform technique(Freeman and Tesar, 1988).

$$\underline{T}_a = [I_{au}^*]\,\dot{\underline{u}} + \dot{\underline{u}}^T[P_{auu}^*]\,\dot{\underline{u}} \tag{11}$$

where

$$[I_{au}^*] = [I_{aa}^*][G_u^a] \tag{12}$$

$$[P_{auu}^*] = [I_{aa}^*] \circ [H_{uu}^a] + [G_u^a]^T[P_{aaa}^*][G_u^a]. \tag{13}$$

'$\circ$' denotes a generalized dot product. $[I_{au}^*]$ represents the effect of the end effector acceleration on the force at the set of minimum coordinate, while $[P_{auu}^*]$ represents the effect of the end effector velocity on the forces at the set of minimum coordinate.

The dynamic model representing the relationship between the actuating joint vector and the oprational velocity/acceleratin vector is obtained from

$$\begin{aligned}\underline{T}_A &= [G_A^u]^T\underline{T}_u = [G_A^u]^T[G_u^a]^T\underline{T}_a \\ &= [I_{Au}^*]\,\ddot{\underline{u}} + \dot{\underline{u}}^T[P_{Auu}^*]\,\dot{\underline{u}}\end{aligned} \tag{14}$$

where

$$[I_{Au}^*] = [G_A^u]^T[G_u^a]^T[I_{au}^*] \tag{15}$$

$$[P_{Auu}^*] = ([G_A^u]^T[G_u^a]^T) \circ [P_{auu}^*]. \tag{16}$$

4. Dynamic Design Index

Seven design indices are considered for the dynamic optimal design, and they are obtained from the dynamic models of Eq. (11). The maximum eigenvalue of $[I_{au}^*]$ is considered first, and quoted as λ_I. The larger λ_I, the larger actuating force is needed for unit operational acceleration. The global maximum eigenvalue index implies the average of the maximum eigenvalue over the entire workspace, and is defined as

$$\Lambda_I = \frac{\int_W \lambda_I \, dW}{\int_W dW} \tag{17}$$

where W means workspace area. The design objective is to minimize Λ_I.

The isotropic index of $[I^*_{au}]$ is defined as

$$\sigma_I = \frac{\lambda_{min}}{\lambda_{max}} \tag{18}$$

where λ_{max} and λ_{min} are the maximum and minimum eigenvalues of $[I^*_{au}]$, respectively. The global isotropic index representing the average of the isotropic index over the entire workspace is defined as

$$\Sigma_I = \frac{\int_W \sigma_I \, dW}{\int_W dW} \tag{19}$$

As the isotropic index of $[I^*_{au}]$ approaches unity, the acceleration capability becomes uniform in all operational directions. The design objective is to maximize Σ_I.

Another design index showing the velocity capacity of the robot system is obtained from $[P^*_{auu}]$. $[P^*_{auu}]$ has two planes for a two degree-of-freedom system. The average of maximum eigenvalues of two planes is defined as

$$\lambda_P = \frac{1}{2} \sum_{i=1}^{2} (\lambda_i)_{max} \tag{20}$$

where $(\lambda_i)_{max}$ is the maximum eigenvalue of ith plane. The larger λ_P, the larger actuating force is needed for unit operational velocity. Also, the global design index for λ_P is defined as

$$\Lambda_P = \frac{\int_W \lambda_P \, dW}{\int_W dW} \tag{21}$$

Consequently, the objective is determined to minimize Λ_P.

The forth design objective is to minimize the effect of gravity load upon the actuators. The 2-norm of gravity load vector is represented as τ_G, and the global design index is defined as the maximum value of τ_G throughout the workspace, and is given as the form of the following infinity norm

$$T_G = \left\{ \sum^{W} (\tau_G)^{\infty} \right\}^{1/\infty}. \tag{22}$$

The last three design indices are the gradient design indices of the three design indices mentioned above. Gradient design index is considered so that the final design can have even distribution of the dynamic characteristics over the workspace. First, the workspace is divided into rectangular meshes with 0.1 m interval, and the difference of each design index between the adjacent two points is defined as gradient design index. The maximum value of the gradient design index throughout the workspace is defined as the global gradient design index. The smaller the global gradient design index, the better distributed the design index throughout the workspace. So, the design objective is to minimize the global gradient design indices. The global gradient design index(Λ_I^G) for the maximum eigenvalue of $[I^*_{au}]$ is defined as

$$\Lambda_I^G = \left(\sum^{W} | \lambda_I^G |^{\infty} \right)^{1/\infty} \tag{23}$$

where λ_I^G denotes the local gradient design index for λ_I. In a similar fashion, the local gradient design indices for σ_I and λ_P are denoted as σ_I^G and λ_P^G, respectively, and their global gradient design indices are defined as

$$\Sigma_I^G = \left(\sum^{W} | \sigma_I^G |^{\infty} \right)^{1/\infty} \tag{24}$$

$$\Lambda_P^G = \left(\sum^{W} | \lambda_P^G |^{\infty} \right)^{1/\infty}. \tag{25}$$

In order to cope with a multi-criteria based design, we employed the concept of composite design index. Various design indices introduced above are usually incommensurate concepts due to differences in unit and physical meanings, and therefore should not be combined with normalization and weighting functions unless they are transferd into a common domain. As the initial step to this process, preferential information should be given to each design parameter and design index. Then, each design index is transfered to a common preference design domain which ranges from zero to one. Here, the preference given to each design criterion is very subjective to the designer. Preference can be given to each criterion by weighting. This provides flexibility in design.

The dynamic composite design index($DCDI$) which takes into account the above mentioned indices can be obtained as the minimum value of the design indeices at a set of design parameters.

$$DCDI = \min\left\{ \widetilde{\Lambda_I^{\alpha}}, \widetilde{\Sigma_I^{\beta}}, \widetilde{\Lambda_P^{\gamma}}, \widetilde{T_G^{\delta}}, \widetilde{\Lambda_I^{G\varepsilon}}, \widetilde{\Sigma_I^{G\zeta}}, \widetilde{\Lambda_P^{G\eta}} \right\} \tag{26}$$

where the upper tilde mark($\sim$) implies that the index is transfered into the common preference design domain. The upper Greek letters(α, β, *etc.*) represent the degrees of the weighting, and usually large value implies large weighting.

Composite design index is constructed such that a large value represents a better design. If the best preference is given the maximum value, and the least preference is given the minimum value of the criterion, the global isotroic index of $[I^*_{au}]$ will be expressed as

$$\widetilde{\Sigma_I} = \frac{\Sigma_I - (\Sigma_I)_{min}}{(\Sigma_I)_{max} - (\Sigma_I)_{min}}. \tag{27}$$

If the best preference is given the minimum value, and the least preference is given the maximum value of the criterion, $\widetilde{\Lambda_I}$ will be expressed as

$$\widetilde{\Lambda_I} = \frac{(\Lambda_I)_{max} - \Lambda_I}{(\Lambda_I)_{max} - (\Lambda_I)_{min}}. \quad (28)$$

And $\widetilde{\Lambda_P}$, $\widetilde{\Gamma_G}$, $\widetilde{\Lambda_I^G}$, $\widetilde{\Sigma_I^G}$, and $\widetilde{\Lambda_P^G}$ are obtained as the same fashion of Eq. (28). The decision of the preference level on the maximum and minimum values is subject to the designer's choice.

5. Dynamic Optimal Design

Mass of link, position of mass center, mass moment of inertia, *etc.* can be cited as dynamic design parameters of manipulator. Figure 3 shows the dynamic parameters of the robot module. In this paper, the dynamic design parameters considered for the dynamic optimal design are m_1, r_1, and r_2. We assume that the links of the manipulator have the shape of hollow cone and have uniform mass density. Then, variations of r_1 and r_2 result in the change of mass moment of inertia and the position of mass center(L_c) of each link. Two constraints are given in the design, as

$$r_1 + R_1 = 0.10\ m$$
$$r_2 + R_2 = 0.10\ m \quad (29)$$

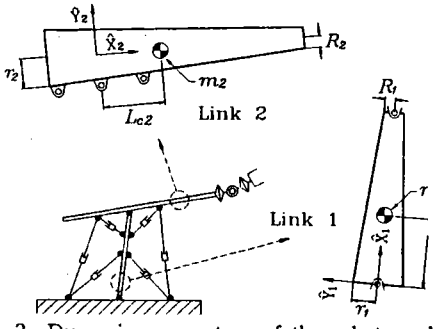

Fig. 3 Dynamic parameters of the robot module

R_i and L_{ci} decrease as r_i increases, and this transition results in the reduction of the gravity and inertial loads at the actuators. The mass moment of inertia with respect to mass center is maximum when r_i is equal to R_i, and the mass moment of inretia decreases as the difference of r_i and R_i increases. Dynamic characteristics of manipulator will also vary by changing the ratio between m_1 and m_2. With the following constraint equations

$$m_1 + m_2 = m_{total} = 15.0\ kg, \quad (30)$$
$$4.0\ kg \le m_1 \le 11.0\ kg \quad (31)$$
$$0.03\ m \le r_1,\ r_2 \le 0.07\ m. \quad (32)$$

a small m_1 results in a large m_2, and consequently large actuator capacity is needed to withstand the increased inertial load. The data for Eqs. (29) ~ (32) are determined based on KIRO-4 robot(Lee et al., 1993) which has been developed in the Department of Precision Engineering and Mechatronics at KAIST(Korea Advanced Institute of Science and Technology).

The kinematic parameters of the manipulator to be used in the dynamic optimization are obtained from the kinematic optimization procedure by the present authors(Lee *et al.*, 1994), and the shape of the manipulator is shown in Fig. 4. To deal with a nonlinear optimization with constraints, three numerical methods are used. The exterior penalty function method is employed to transform the constrained optimization problem into an unconstrained optimal problem. Next, Powell's method is applied to obtain an optimal solution for the unconstrained problem, and quadratic interpolation method is utilized for uni-directional minimization(Yuan-Chou, 1985).

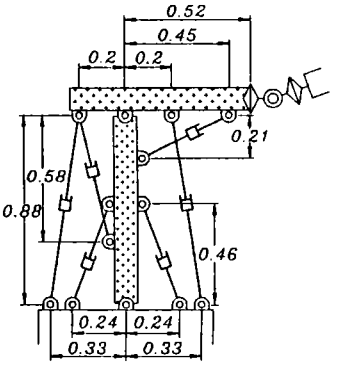

Fig. 4 Kinematic parameters of the initial dynamic design. (Unit is meter.)

Various optimization results can be obtained by changing weighting factors for each design index. Based on the result, the relationships between the optimal design parameters and the design indices can be understood. The dynamic optimization results for the case when only one weighting factor is set to unit with the others set to zero are illustrated in Table 1, from Case 1 through Case 7. The Greek letters in the table denote the weighting factors for each design

Table 1 Dynamic parameters of optimization results

Design Cases	Dynamic Design Parameters		
	m_1	r_1	r_2
Case 1 : Only α is unit	11.00	0.070	0.030
Case 2 : Only β is unit	4.00	0.070	0.030
Case 3 : Only γ is unit	11.00	0.070	0.050
Case 4 : Only δ is unit	11.00	0.070	0.065
Case 5 : Only ε is unit	11.00	0.070	0.030
Case 6 : Only ζ is unit	11.00	0.030	0.070
Case 7 : Only η is unit	11.00	0.070	0.030
Case 8 : All weighting factors are units	7.98	0.070	0.050
Case 9 : β is 0.5 Others are units	9.98	0.061	0.030
Case 10 : β is zero Others are units	11.00	0.070	0.031

index. Figure 5 shows the shapes of the optimized module for each design case. The case with higher density of dots represents a bigger mass.

In the design of robot manipulator, a special concern has been paid to reduction of gravity load. The Case 4 of Table 1 corresponds to the design considering only the reduction of gravity load. The actuator loads due to gravity load will be reduced in this case. On the other hand, in Case 2 mass is concentrated on link 2 as compared to the other cases. Thus, large actuator capacity will be required. In other word, a global isotropic characteristic can be obtained with sacrifice of large actuator effort.

In order to evenly satisfy the design objectives for all design indices, all of the weighting factors are set to unit. The optimization results for this design are shown in Case 8 of Table 1 and Fig. 5 (h).

Here, the results of Case 1 through Case 8 are compared with respect to their actuator sizes. Optimal actuator sizes are evaluated with respect to the required operational specifications, such as maximum load handling capacity, maximum hand velocity and maximum hand acceleration(Yuan-Chou, 1985). Maximum load handling capacity is obtained on the basis of Eq. (8), while maximum hand velocity and

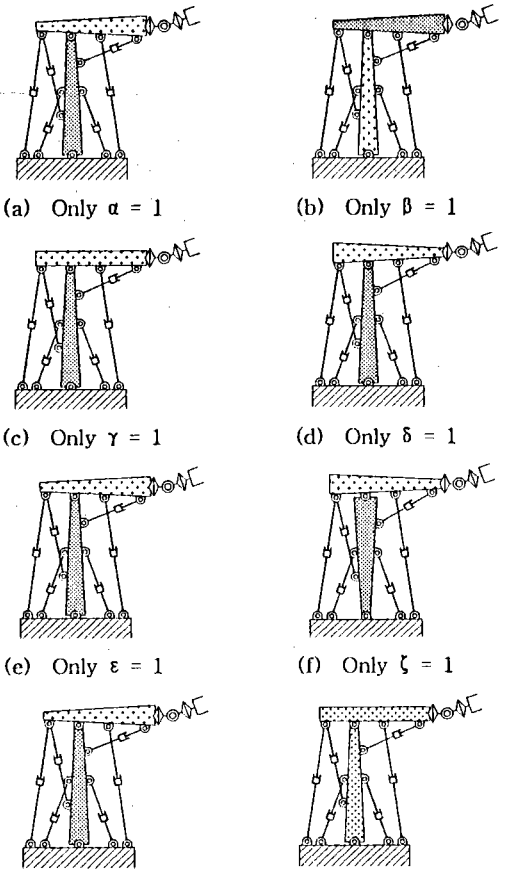

(a) Only $\alpha = 1$ (b) Only $\beta = 1$

(c) Only $\gamma = 1$ (d) Only $\delta = 1$

(e) Only $\varepsilon = 1$ (f) Only $\zeta = 1$

(g) Only $\eta = 1$ (h) All weights are units

Fig. 5 Schematic diagram of the dynamic optimization results

Table 2 Optimal actuator sizes for specified maximum load handling capacity

Maximum load handling capacity : 100.0 *N*				
Actuator numbers	Acuator sizes (Unit is Newton)			
	Design A	Design B	Design C	Design D
a_1	243.6	256.5	252.4	246.0
a_2	323.4	341.5	336.8	329.3
a_3	242.6	250.9	246.4	241.8
a_4	286.6	300.7	294.7	287.7
a_5	143.2	155.0	151.3	146.1
a_6	278.9	294.0	290.3	284.1

Table 3 Optimal actuator sizes for specified maximum hand velocity

Maximum hand velocity : 0.70 *m/s*				
Actuator numbers	Acuator sizes (Unit is Newton)			
	Design A	Design B	Design C	Design D
a_1	73.1	90.1	84.2	76.7
a_2	82.1	102.2	95.5	86.8
a_3	90.2	90.3	84.9	82.4
a_4	107.8	123.0	115.1	107.0
a_5	64.3	64.3	60.1	58.2
a_6	57.5	60.6	56.9	54.3

Table 4 Optimal actuator sizes for specified maximum hand acceleration

Maximum hand acceleration : 0.70 m/s^2				
Actuator numbers	Acuator sizes (Unit is Newton)			
	Design A	Design B	Design C	Design D
a_1	63.0	78.9	74.0	67.0
a_2	71.2	89.9	84.3	76.0
a_3	87.7	88.3	83.1	80.6
a_4	100.7	116.7	109.7	101.8
a_5	55.5	57.5	54.2	52.1
a_6	55.4	58.3	54.9	52.5

acceleration are obtained on the basis of Eq. (14). Tables 2, 3, and 4 illustrate the optimal actuator sizes for each case. Design A represents the case that only gavity loads are considered, and Design B represents the case that all of the weighting factors are set to unit. Design A has the least actuator sizes, and the actuator sizes for Design B are larger than those of Design A. This is due to the effect of the isotropic index included in the composite design index.

Now, the effect of the isotropic index on the result of dynamic optimization is invesigated by varying the weighting factor for the isotropic index. Listed in Case 9 and Case 10 of Table 1 are the optimization results for the weight of the isotropic index to be 0.5 and zero, respectively, with the other indices to unit. It is

shown that the mass of link 1 increases, as the weight for the isotropic index decreases. The actuator sizes for these design cases are illustrated in Table 2, 3, and 4. Design C represents the case that the weight of the isotropic index is 0.5, and Design D represents the case that the weight of the isotropic index is zero with the other weights set to unit. As expected, actuator sizes become smaller as the weight of isotropic index approaches zero.

From the above analysis based on actuator sizes, we could observe that there exists a trade-off between the isotropic characteristics and the actuator sizes. Composite design index employed in this work could provide a flexible design methodology with consideration of weighting factors for several design indices, even if conflicts exist among some design indices.

6. Conclusion

In this study, the dynamic optimization of a two degree-of-freedom anthropomorphic robot module with redundant actuation was performed. The results of dynamic optimization show enhancement of dynamic characteristics, as compared to those of kinematic optimization. The relationship between the dynamic parameters and the dynamic design indices introduced in this work was analyzed. It was shown that a trade-off exists between the isotropic characteristic and the actuator sizes. Composite design index was employed to deal with a multi-criteria based design, and also allow flexible design by varying the weights for each design index.

Reference

Freeman, R.A. and Tesar, D. (1988). Dynamic modeling of serial and parallel mechanisms/robotic systems, part I-Methodology, part II-Applications, *Proc. 20th ASME Biennial Mechanisms Conf* Orlando, FL, DE-Vol. 15-3, pp. 7-27.

Hogan, N. (1985). The mechanics of multi-joint posture and movement control, *Biological Cybernetics*, Vol. 52, pp. 315-331.

Kang, H.J., Yi, B-J., Cho, W., and Freeman, R.A. (1990). Constraint-embedding approaches for general closed-chain system dynamic in terms of a minimum coordinate set, *The 1990 ASME Biennial Mechnism Conf*, Chicago, IL, DE-Vol.24, pp. 125-132.

Lee, D.G., Jeong, K.S., Kim, K.S. and Kwak, Y.K. (1993). Development of the anthropomorphic robot with carbon epoxy composite materials, *Composite Structures*, Vol. 8, No. 5, pp. 644-651.

Lee, S.H., Yi, B-J. and Kwak, Y.K. (1994). Optimal design of closed-loop type robot module with redundant actuation, *2nd IFAC/IFIP/IFORS Workshop on Intelligent Manufacturing System*, Vienna, pp. 569-573

Park, H.S. and Cho, H.S. (1991). General design condotions for an ideal robotic manipulator having simple dynamics, *Int. J. Robotics Research*, Vol. 10, No. 1, pp. 21-29.

Singh, J.R. and Rastegar, J. (1992). Optimal Synthesis of Robot Manipulators Based on Global Dynamic Parameters, *Int. J. of Robotics Research*, Vol. 11, No. 6, pp. 538-548

Spence, P.A. (1986). *Basic human anatomy*, The Benjamin/Cummings Publishing Co. Inc., 2nd Ed.

Yi, B-J. and Freeman, R.A. (1991). Modeling and control of impedance properties in biomechanical systems, *Proc. ASME WAM, Advances in bioengineering*, Atlanta, GA, BED-Vol. 20, pp. 521-524.

Youcef-Toumi, K. and Asada, H. (1987). The design of open-loop manipulator arms with decoupledand configuration-invariant inertia tensors, *ASME J. Dynamic systems, Measurement, and Control*, Vol. 109, pp. 268-274.

Yuan-Chou, B.C. (1985). *Computer-aided optimization in the dynamic analysis and parameteric design of robotic manipulators*, Ph.D. Dissertation, University of Florida, Gainsville.